March 2000 • NREL/SR-520-27960

Subcontractor Report

Photovoltaic Manufacturing Technology Monolithic Amorphous Silicon Modules on Continuous Polymer Substrates

Final Technical Report
July 5, 1995 — December 31, 1999

F. Jeffrey
Iowa Thin Film Technologies
Boone, Iowa

National Renewable Energy Laboratory
1617 Cole Boulevard
Golden, Colorado 80401-3393

NREL is a U.S. Department of Energy Laboratory
Operated by Midwest Research Institute • Battelle • Bechtel

Contract No. DE-AC36-99-GO10337

March 2000 • NREL/SR-520-27960

Photovoltaic Manufacturing Technology Monolithic Amorphous Silicon Modules on Continuous Polymer Substrates

Final Technical Report
July 5, 1995 — December 31, 1999

F. Jeffrey
Iowa Thin Film Technologies
Boone, Iowa

NREL Technical Monitor: R.L. Mitchell

Prepared under Subcontract No. PV006101

National Renewable Energy Laboratory
1617 Cole Boulevard
Golden, Colorado 80401-3393

NREL is a U.S. Department of Energy Laboratory
Operated by Midwest Research Institute • Battelle • Bechtel

Contract No. DE-AC36-99-GO10337

Available electronically at http://www.doe.gov/bridge

Available for a processing fee to U.S. Department of Energy
and its contractors, in paper, from:
U.S. Department of Energy
Office of Scientific and Technical Information
P.O. Box 62
Oak Ridge, TN 37831-0062
phone: 865.576.8401
fax: 865.576.5728
email: reports@adonis.osti.gov

Available for sale to the public, in paper, from:
U.S. Department of Commerce
National Technical Information Service
5285 Port Royal Road
Springfield, VA 22161
phone: 800.553.6847
fax: 703.605.6900
email: orders@ntis.fedworld.gov
online ordering: http://www.ntis.gov/ordering.htm

Printed on paper containing at least 50% wastepaper, including 20% postconsumer waste

TABLE OF CONTENTS

Executive Summary

Iowa Thin Film Technologies is completing a three phase program which has increased throughput and decreased costs in nearly all aspects of its Thin Film photovoltaic manufacturing process. The overall manufacturing costs have been reduced by 61 percent through implementation of the improvements developed under this program.

Development of the ability to use a 1 mil substrate rather than the standard 2 mil substrate results in a and 50 percent cost-saving for this material.

Process development on a single pass amorphous silicon deposition system have resulted in a 37 percent throughput improvement.

A wide range of process and machine improvements have been implemented on the TCO deposition system. These include detailed parameter optimization of deposition temperatures, process gas flows, carrier gas flows, and web speeds. An overall process throughput improvement of 275 percent was achieved based on this work.

The new alignment technique was developed for the laser scriber and printer systems which improved registration accuracy from 100 microns to 10 microns. The new technique also reduced alignment time for these registration systems significantly. This resulted in a throughput increase of 75 percent on the scriber and 600 percent on the printer.

Automated techniques were designed and implemented for the module assembly processes. These include automated busbar attachment, roll based lamination, and automated die cutting of finished modules. These processes were previously done by hand labor. Throughput improvements ranged from 200 percent to 1200 percent relative to hand labor rates.

A wide range of potential encapsulation materials were evaluated for suitability in a roll lamination process and for cost-effectiveness. A combination material was found which has a cost that is only 10 percent of the standard EVA /Tefzel® cost and is suitable for medium lifetime applications. 20 year lifetime applications still require the more expensive material.

1.0 INTRODUCTION

This FINAL TECHNICAL REPORT has been prepared under Subcontract ZAF-5-14271-04 (Mod. 12) with the Midwest Research Institute National Renewable Energy Laboratory Division. This Final Technical Report covers the performance period of July 5, 1995 through December 31, 1999.

1.1 Background

The Department of Energy (DOE), in cooperation with the U.S. photovoltaic (PV) industry, has the goal of enhancing the U.S. PV industry leadership in the world market. To further this goal, the Photovoltaic Manufacturing Technology (PVMaT) project was initiated in FY 1991 to assist U.S. industry in the improvement in module manufacturing processes and the substantial reduction of module manufacturing cost. PVMaT's partnership with industry is being implemented in phased procurements to support continued progress as each phase accomplishes its objectives. Phases 1, 2, and 3 have been successfully implemented beginning with Phase 1 in 1991.

Phase 4A, the PVMaT addressed in this subcontract, addresses areas of research and development including issues related to cost-effective PV end-products, including module manufacturing, flexible manufacturing approaches, systems integration, and balance of systems. This subcontract represents an R&D in approach under Phase 4A2, Product Driven PV Module Manufacturing Technology, and is planned as a three year effort. It is directed toward R&D on PV module manufacturing process technology (with no funding for acquisition of production line equipment).

During this Phase 4A2 subcontract, Iowa Thin Film Technologies, Inc. (ITF) was to focus on increasing the throughput of their metalization, a-Si deposition, laser-scribing and welding processes and on reducing the overall module manufacturing costs on the ITF production line by 68%. Efforts to accomplish these goals will be focused on replacing the ITF TiN layer with a less absorbing layer ZnO layer; investigating alternate sources for the supply of Zn and O in the ZnO growth process; designing and implementing a web steering system machine control programs; identifying new laser operating parameters to optimize the laser beam scan speed and study alternative processes for the scribing; developing a new water-based insulating ink printing and roll based laminating processes for the ITF production line; designing and implementing baffles for the isolation of deposition regions; studying alternative methods of welding shunts in cell-interconnects; and automating the final process steps of busbar attachment and web cutting.

1.2 Objectives

The objective of this subcontract over its three year duration is to improve overall module performance, increase the throughput of the metalization, a-Si deposition, laser-scribing, and welding processes and to reduce the overall module manufacturing costs of the ITF production line by 68% from baseline.

1.3 Approach

Efforts toward meeting the goals of this program were divided into the following five main categories:

- Deposition Process
- Improvements in Laser and Printing Process Throughput
- Substrate Cost Reduction
- Busbar Attachment and Web Cutting Automation
- Reduction in Encapsulation and Module Assembly Costs

Program accomplishments are described below organized under these five categories.

2.0 PROGRAM ACTIVITIES AND ACCOMPLISHMENTS

2.1. Deposition Process

Single Pass Tandem Silicon Deposition Machine

A new single pass tandem machine was brought on line during this project. Deposition rates and uniformity were optimized for each of the six deposition zones independently and then, jointly, for a complete tandem device. Currents and fill factors are slightly better than for tandem devices made by passing a web through the single junction machine twice. This might be expected because there is no air exposure between the two device depositions. However, device voltage was initially lower than it was from the previous system. Voc also dropped over the length of the run.

The majority of the low voltage effect was determined to be poor thermal control of the p+ deposition boxes. It was observed that: first, the web temperature varied significantly from the platen temperature and second, this variation changed with time over the length of the run. To control temperature it was necessary to install cooling on the P-box. Once control over the P-box temperature was established, it was possible to establish a correlation between web temperature and platen temperature. This correlation is now used to set the platen temperature. The set point is altered during the length of the run to maintain a constant temperature at the web.

Some temperature drift was also observed in the I-box. A similar correlation and correction procedure was established for this box.

Gas flow rates and RF powers were re-calibrated based on the new temperatures to insure that current levels in the top and bottom devices remain matched.

An overall increase in throughput of 37% was achieved for the a-Si deposition process as a result of the optimization process.

Improved Metalization and ZnO TCO Process Throughput

Metalization The metalization consists of a stack of sputtered stainless steel and aluminum layers which act as a back reflector and current collector. The metalization process consisted of three separate steps. The first step is the de-watering/de-gassing of the web material. This allows the web to release volatile impurities which would interfere in subsequent processing steps and stabilizes the mechanical and thermal properties of the polyimide, without web distortion or damage. The second step is the sputter deposition of the metal base layer and reverse side anti-static coat. This results in a metal deposition with a conductivity of less then 1 ohm per square. The third step is a sputter deposition of titanium nitride (TiN) which acts as a diffusion barrier between the metal and the silicon. It was important that all of these processes were completed without causing scratching to the web surfaces or contaminating the surface of the web with particles.

ITF intended to increase the throughput of the metalization by designing and implementing an isolation baffle system to allow all processes to be carried out on a single pass basis. It has been determined that during the metal deposition the partial pressure of contaminant gases (including nitrogen, oxygen, and water) must be below $2x10^{-5}$ torr. Given the pressures and gas flow for the various operations, isolation between the de-gas process and the metal deposition would need to be greater then three orders of magnitude. Isolation between the TiN and metal would need to be greater then two orders of magnitude. The size of the chamber(s) and cost of implementing rotary slits and differential pumping to obtain the required isolation, as well as being able to pass the web through such a system without scratching the surfaces, makes such modifications prohibitively expensive. Therefore, building separate vacuum systems for each operation becomes the economically feasible choice.

ITF has designed constructed a new vacuum system to operate as the de-gas system. This will allow for simultaneous operation of both the de-gas and metal deposition. It will also remove the raw web from an environment that generates large quantities of particulates which are attracted to the surfaces by static charge thus contaminating it and causing shunting in the final devices. The metal and TiN deposition will remain in the same chamber and these processes will be operated sequentially. Throughput remains limited by the heat removal from the targets, by the power output capacities of the power supplies and by the mechanics of the web drive units. Moving to the new two-chamber operating procedure increases throughput by 37%.

ZnO TCO The transparent conducting oxide (TCO) layer consists of a chemical vapor deposited zinc oxide (ZnO) which acts as a current collector on the top of the solar cell device while allowing light to pass through to the silicon layers below. It is important that the ZnO TCO is transparent to light, with less then 10 ohms per square resistivity, has a good electrical contact to the silicon, and adheres to the silicon surface.

It was ITF's intention to increase the throughput of the roll-to-roll ZnO TCO deposition system by ascertaining the importance of each step of the process: substrate temperature; increasing the diethyl zinc (DEZ) flow rate; variation of the dopant feed stock; and modification of the inflow gas manifold.

A full study of rate versus temperature was carried out for rate optimization.

The flow rates of the reactant vapors were investigated. The introduction of the reactants is accomplished by using a carrier gas that is passed through a bubbler system. Therefore, the bubbler temperature, pressure, and carrier gas flow rates are critical factors to consider. It was found that the optimum ratio of the water to DEZ vapor ratio is 2.16 to 1. The properties of the ZnO film were somewhat insensitive to the level of dopant flow. Too much dopant cause stress fracturing of the film while too little caused higher resistivities. However, the window of acceptable flows was quite large. Modification of the inflow gas manifold by reducing the flow restriction at the jets improved the deposition rate and also helped to prevent premature clogging of the openings.

ITFT has implemented these changes into the manufacturing process and has increased the throughput to higher levels for this process. An overall throughput increase of 200% was achieved under this program.

Roll Based Deposition Throughput Improvement for Back Contact Layer

The back contact layer consists of a sputtered metal stack with a titanium nitride (TiN) top coating which acts as a diffusion barrier between the metal and the silicon. Although TiN is a good diffusion barrier, it has poor optical properties when used as the back contact for silicon solar cells resulting in absorption of light at the metal/silicon interface.

A significant effort was aimed at back reflector improvement. Fabrication parameters and techniques were sought to allow replacement of the current TiN layer with a ZnO layer sputtered from a metal target. The goal was to produce a ZnO layer with less than 3% absorption to replace the TiN layer leading to a device current improvement of 25% to 35%.

Total reflectance of light from the back contact and back contact texture are both critical to achieving the highest efficiency of collection of red light. High total reflectance minimizes loss of light by absorption at the back surface and texture provides scattering. Scattering increases the path length before reaching the front surface and creates the possibility of total internal reflection of light when it reaches that surface. In addition to the optical performance, the back contact must also be stable and have a good mechanical bond to the substrate.

In order to guarantee the best reflectance and optimum scattering, it is important to have a characterization method. To establish a capability of monitoring texture during processing within the deposition chamber, a system was constructed which uses a laser diode along with 4 silicon detectors at fixed angular positions. This system provided 4 data points to be used to monitor the efficiency of scattering of red light.

Initially, a zinc 2% aluminum target was installed in the PTS for deposition onto a polyester web. Polyester was used because it is transparent to the light wavelengths of interest and allows for transmission spectra tests. Zinc oxide is deposited from a metal target using a reactive sputtering technique in an argon/oxygen atmosphere. Various pressures and argon/oxygen ratios were investigated. Deposition was controlled at 400 watts power, web speed at 2 inches/min. and with no applied heating.

Laboratory scale results have shown that the ZnO layer incorporated between the back metal contact and the n+ layer can significantly enhance reflection and therefore the collection efficiency of red light. To date, ITF has been unable to incorporate this in our roll based pilot manufacturing line. Attempts to incorporate a sputtered ZnO layer have resulted in shunted cells or a very high leakage current while CVD ZnO has produced a barrier.

A wide range of experiments were carried out to determine the source of the shunts. Deposition temperature, power and ZnO film thickness were varied and devices examined for correlations between these parameters and shunt level. No correlation was found. An amorphous n+ layer was substituted for the standard microcrystalline layer to investigate the possibility that the high deposition power and H2 etching associated with the microcrystalline layer were causing damage. A range of deposition powers and doping levels were used for the amorphous n+ layer. No reduction of shunt level was seen with these changes. To further investigate the effect of the interface with the silicon layer, a TiN layer was deposited over the ZnO layer as a barrier before fabrication of the silicon layers. This configuration was shown to have shunts also.

During the course of these experiments, one correlation was observed: the shunt level increased with the occurrence of physical damage that results from poor handling. While this is true for all substrate combinations, the sensitivity seemed much higher for the ZnO coated back material. It may be that the mechanical strength or interface bonding strength of the ZnO is sufficiently lower than the TiN that the ZnO is susceptible to mechanical damage. This weakness would be more noticeable on our flexible substrate than on a more rigid material.

2.2. Improvements in Laser and Printing Process Throughput

Several improved sensors were evaluated, and candidates selected and implemented to speed up web registration under computer control. This included the development of new software to incorporate the improved detectors into the alignment process and some redesign of laser and printer platens. ITF examined photoelectric detectors, linear arrays and position sensor detectors for use in registration mark positioning. Resultant detection schemes and alignment processes were incorporated into the printer and laser scriber in the ITF production line processes steps.

Several alignment detector technologies were evaluated and the best candidate was selected for the computer system currently controlling the web drive. New laser operating parameters to optimize laser beam scan speed were established. In addition, the laser scriber was optimized for maximum throughput in conjunction with the detectors and software. Hardware changes such as stepper motor and gearing changes were evaluated for their potential for reducing overall process time.

This effort over the contract period resulted in a throughput improvement of 75% for the laser system and 600% for the printer system.

Throughput improvements with the roll-to-roll laser scriber/welder and screen-printing modules are determined by a) improvement in submodule alignment and b) improvements in unit submodule processing time.

The scriber and printer have similar alignment technologies, both in hardware and software used. Common to both scriber and printer are stepper and servo motors for web motion over a platen and fiber optic sensors. The scriber probes are mounted on an x-y stage that aligns with and moves relative to the web on the scribing platen. Previously, the printer screen had been hand adjusted to maintain alignment with the web. However, under this development contract, the screen printer was mounted on an x-y stage that automatically aligns with and moves relative to the web on the printing platen. The software for the web movement, stage/screen movement, and fiber optic detector registration is also similar for the scriber and printer. There exists a great variety of optical detection schemes for web alignment. They vary greatly in complexity and cost, ranging from over $20,000 for CCD camera systems to as little as $100 for fiber optic sensors. All claim resolutions smaller than 0.02 mm (1 mil). In each of these systems, the registration capability is dependent on the accuracy of the mechanical system integration and alignment. For optical systems, the smaller the resolution, the smaller the depth of focus, which is a source of concern with a moving bouncing web. Thus the final decision for an improved sensor was made along with how the final mechanical registration was to be achieved.

For the laser scribing system, a solution was found with a transmission fiber optic system using proprietary improvements. Previously, the resolution was 0.025 mm, but suffered from fiber optic light scattering caused by ZnO crystallite diffraction in the region of the registration mark. This resulted in a final registration reproducible only to 0.15 mm with the standard fiber optic system. Several improvements to the fiber optic system were evaluated. Figure 1 shows a graph showing a comparison of the position resolution of the final improved system with the original system. This graph indicates that a registration of 0.02 mm should be possible with a 0.5 fiber light intensity resolution. This new system achieves routine registration 0.05 mm. This larger value is not caused by the intensity resolution. Investigation has shown that the registration marks are not parallel lines. As can be seen in the micrograph, Figure 2, there was an oscillation

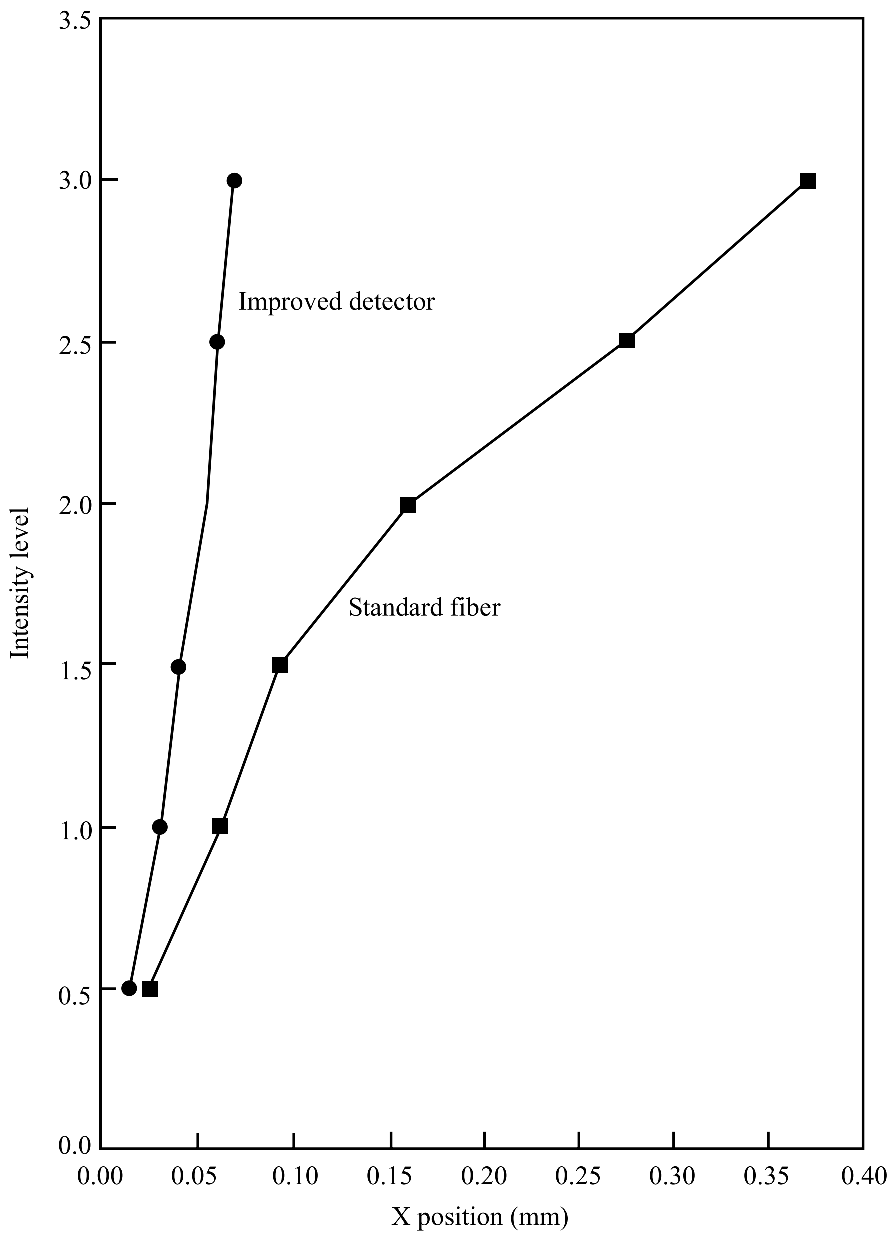

Figure 1.   Comparison of standard and improved fiber optic detectors. (prepared by M. Noack)

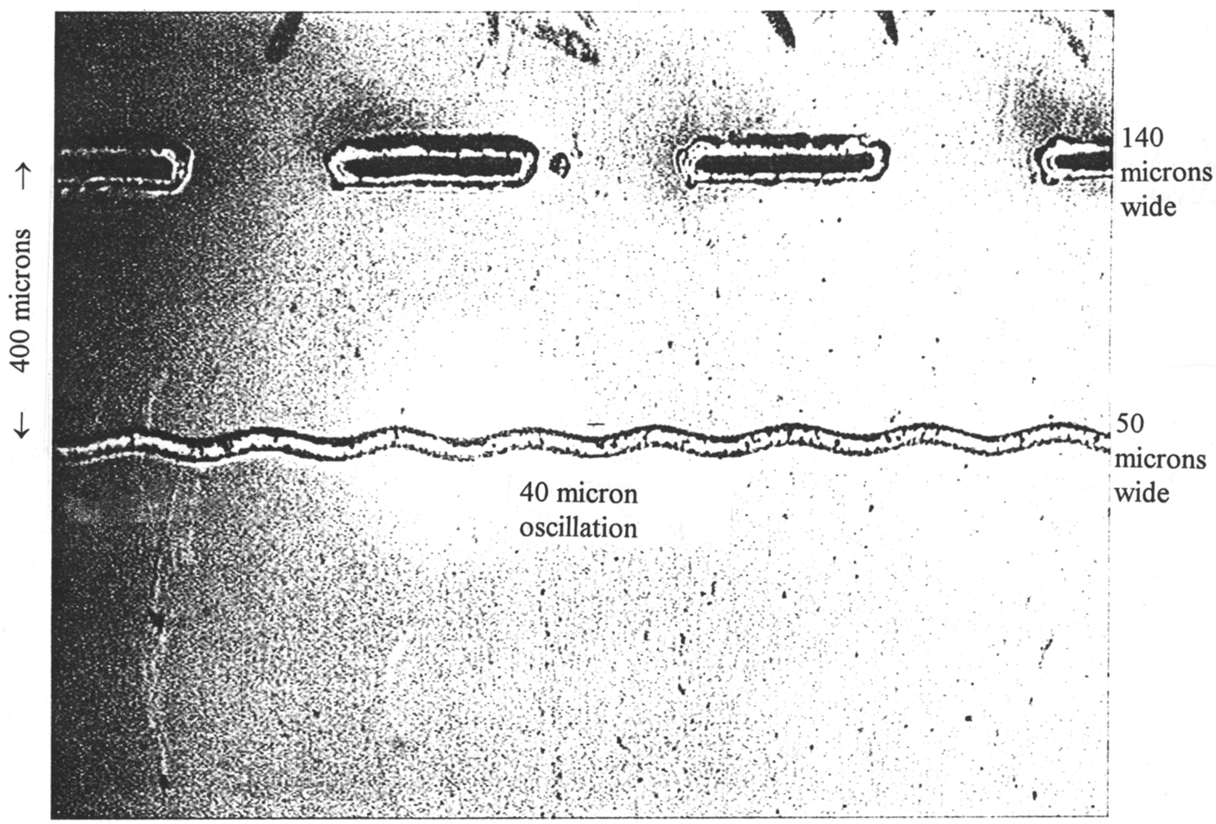

Figure 2. Micrograph of laser scribe lines showing "worst case" oscillation.

present that could be as large as 0.040 mm. It is believed that this oscillation limited our original registration reproducibility to the 0.05 mm value. The oscillation is caused by mechanical resonance with x-y stage and presently has been greatly reduced by mechanical damping to a massive wall structure. Improvements in limiting damping in future scriber systems will involve: 1) using high precision x-y tables, 2) massive support structures, and 3) coupling the support structures to a massive wall for additional damping.

The present scribing parameters for the initial through scribe are 2.6 kHz, 65 mm/sec and 1.0W. The present parameters for the weld scribe are 2.6 kHz, 20 mm/sec and 1.25W. The present parameters for the TCO cut are 5.0 kHz, 65 mm/sec and 0.75 W.

For the printer system, registration reproducibility was limited by non-uniform advancement of the web, or "hopping." Nevertheless, the improved fiber-optic system was incorporated with the baseline printer system resulting in marked improvement in registration (+/- 0.05 mm). With the completion of the x-y mechanical screen registration mentioned above, an alignment of +/- 0.02 mm (1mil) was achieved. Alignment of printed pattern to the scribed pattern has a resolution of +/- 10 micron and a reproducibility of +/- 25 micron.. The screen alignment equipment has x, y, theta adjustment, screen lift-up during web transport, and anti-lash spring tensioning of the screen motion. Registration mark detection is done with precision scribe-line sensors.

Table 1 below presents a list of sources for alignment errors for the scriber and printer for original (pre-contract) and present (post-contract) alignment accuracies. Decreases in scribed line variations were the result better x-y stages and more massive mountings. Present decreases in printer web hop are due to platen vacuum modifications.

The preceding discussion on approaches to improve web alignment accuracy and speed is summarized in Table 2. The final improvements are presently operational on the scriber and on the printer.

Additional improvements in printer process throughput were obtained by reducing the percentage area loss due to the cell interconnect area and silver ink current collecting finger area. The base (pre-contract) and present (post-contract) percent area loss due to interconnect and finger grids is summarized in Table 3. Throughput is improved by reducing this "dead" area because the power per unit aperture area increases for constant web linear throughput speed in the printer.

An additional improvement made in the printer system was the implementation of automated sideways tracking and registration to the web edge. This precise sideways printer alignment was required for the automated die-cutting also developed under this contract. The method employed was to register the printing screen to the side or edge of the web, using two fiberoptic etectors. The two detectors, operating in the reflection mode, were spaced closely to each other (within 0.5 mm), and the web edge is intended to lie <u>between</u> the two edge detectors. When the signal from
the "outside" detector (the detector furthest from the web center) shows no reflected signal, <u>and</u> the signal from the "inside" detector (the detector closest to the web center) does show a reflected

signal, the web edge is determined by the computer code to be aligned properly relative to the screen. If both detectors show no reflected signal, they (and the screen) are too far from the web center, and the code adjusts the detectors and screen until the inside detector shows reflection and the outside detector does not. If both detectors do show a reflected signal, they (and the screen) are too close to the web center, and the detectors and screen are adjusted accordingly.

Table 1. Sources of alignment errors for the scriber and printer for original, current, and expected accuracies.

Sources of Alignment Errors

Scriber

	Web Hop	**Head Location**	**Line Wobble**	**Line Bow**	**Line Spread**
Original	+/-0.1 mm	+/-0.01 mm	+/-0.02 mm	+/-0.025 mm	+/-0.05 mm
Present	- -	+/-0.01 mm	+/-0.01 mm	+/-0.01 mm	+/-0.01 mm

Printer

	Web Hop	**Screen Stretch**	**Screen Location**
Original	+/-0.1 mm	+/-0.05 mm	- -
Present	--	+/-0.02 mm	+/-0.01 mm

Table 2. Approaches to improved web alignment and speed.

ORIGINAL PROCESS PLAN
• Advance web to alignment position • Web motion stopped when led detector triggered ➔Slow process. Response time limits accuracy
⇓
FIRST ALTERNATIVE APPROACH
• Advance web to alignment position • Wide field detector watches approach, slows web near end ➔Faster and more accurate process ➔Still limited by web “hop”
⇓
IMPROVED ALTERNATIVE (PRESENT PROCESS)
• Advance web to approximate position and lock down • Processing head is aligned to final web position using LED detectors ➔Excellent processing speed , excellent accuracy ➔Operational on scriber ➔Operational on printer

Table 3. Percent area loss due to interconnect and finger grid areas.

PERCENTAGE AREA LOSS

BASE (STARTING MEASUREMENTS)

Insulator Ink Width:	**.6 mm**	Weld Line Width:	**.8 mm**
Finger Width:	**.7 mm**	Alignment Tolerance:	**.15 mm**

Cell Width	Finger	Interconnect	Total
2 cm	**7%**	**10%**	**17%**
4 cm	**7%**	**5%**	**12%**

PRESENT

Insulator Ink Width:	**.3 mm**	Weld Line Width:	**.4 mm**
Finger Width:	**.4 mm**	Alignment Tolerance:	**.075 mm**

Cell Width	Finger	Interconnect	Total
2 cm	**4%**	**5%**	**9%**
4 cm	**4%**	**2.5%**	**6.5%**

A survey of alternative scribing methods

Of the non-laser methods considered for scribing (mechanical tool or blade; electrochemical; ultrasonic cutting tips), only the mechanical scribing techniques have been used, notably with thin-film PV coatings on glass substrates. [Y. S. Tyan and E. A. Perez-Albuerne, "A Simple, Monolithically Integrated Thin-Film Solar Cell Array," Proceedings of the 16th IEEE PV Specialists Conference, San Diego, CA 1982]. However, there are many steps in the process that require cleaning, handling and scribing before device deposition is completed, which can cause contamination and device damage. Damage to a flexible thin-film module is of special concern because of the potential damage to the polyimide substrate. The device/module fabrication method used by ITFT, termed post-absorber [C. Fredic et al., Proc. of the 23rd IEEE PVSC, Louisville, KY, pp. 437-440, 1993] avoids damage to the back electrode and semiconductor layers.

ITFT is aware of work by others in the solar field using mechanical scribing in PV module processing. Lockheed-Martin personnel have experimented with mechanical scribing (used with weighted tip and laser range finder) to scribe through Mo and Mo/CIS layers on polyimide substrates. (For example, see Vapor Phase Manufacturing of Flexible, Thin-Film CIS Photovoltaics, Quarterly Report #7, 18 July 1997, prepared for DARPA/DSO under consortium agreement MDA972-95-3-0036, Dr. Steven Wax, program monitor. Portions of this report contain proprietary information not for general release without permission of the consortium members and DARPA.) Lockheed-Martin's mechanical scriber was inferior in comparison to their laser scriber for both speed, quality of cuts, and debris avoidance on the soft and flexible polymer substrate [Dr. Tim Gillespie, Lockheed-Martin Corp., Denver, CO, personal communication]. Their choice was to abandon the mechanical scriber in favor of the laser scriber. Even for solar thin-film modules on rigid glass substrates, early attempts at mechanical scribing by various companies have been changed to laser scribing in the manufacturing process. The improvements in laser technology (e.g., diode-pumped YAG lasers) have tipped the balance in favor of laser scribing systems, with their inherent cleanliness, evenness of cut, and narrow cut width. TDK, using a Japanese process that is similar to ITFT's, has opted for laser fabrication of a-Si modules on polymer web.

When techniques other than lasers for welding were considered (electronic or ultrasonic spot-welding techniques) really nothing was found that would surpass laser welding in cleanliness, eveness and resolution of weld-area. The action of a laser beam impinging on a 20 micron thick silver (Ag) ink line printed on top of a 3 micron ZnO + 0.5 micron a-Si + 0.3 micron aluminum (Al) layers causes a Ag-Al silicide to form, where the semiconductor Si is greatly diluted by Ag material.

It is unlikely that the action of other than a laser beam will cause the absorption of energy throughout the Ag-ink/ZnO/a-Si/Al stack in such a way that a conductive junction is formed. Also, the spatial resolution of a 50 micron (0.05mm) diameter laser beam spot allows interconnect areas to be made as narrow as other steps in the process allow; e.g., in our case, three 0.3 mm wide print lines (two insulating ink, one conducting ink) can create a "dead" area under 1mm wide. However, an attempt was made at ITFT to use needle-point electrodes to spot weld both Ag ink and ZnO directly to the Al layers, trying different voltages, currents, and polarities, but the results were unsatisfactory (e.g., resistance higher than by laser welding; charring at point of minimum resistance), and this line of research was discontinued.

The conclusion drawn is that laser scribing and welding are the preferred methods for our cell interconnection. Due to the results of our survey and our own in-house spot-welding attempts, we abandoned plans to modify our equipment for alternatives to laser scribing. Instead, we began a survey of new laser scribing technologies for future expansion of laser scribing facilities (e.g. diode-pumped lasers).

We have gathered literature/information, and obtained quotes from the most promising of more than a dozen diode-pumped pulsed YAG laser manufacturers contacted. For an 8W, 5 kHz, TEM(0,0) system, these lasers range in price from approximately $34K to $100K. This compares with around $20K for a conventional rail-mounted, lamp-powered, Q-switched YAG laser. Originally, it was believed that the high initial cost of diode-pumped lasers would be offset by the reduced operational costs (principally electricity costs) as compared with lamp-powered YAGs. However, the high replacement costs of the pumping diodes (around $4k to $15K every 5,000 to 10,000 hours), will almost double the monthly operation costs of a multi-beam pumped-diode laser system, as compared with our present system. Several distributors have told us that diode-pumped lasers are "shaking down" in price and standardization, similar to what has occurred for UV excimer lasers, and earlier for rail-mounted YAGs. Anticipated time frame for this to occur is about 2 years.

In January, 1999 we obtained a diode pumped, pulsed, 1064 nm YAG laser for testing from a potential vendor. This was a nominal 10W TEM (0,0) unit. Unfortunately, this unit proved to be too unstable at the powers we were examining (a watt or less). The quality of the TEM (0,0) beam did not allow good beam coupling with the result that scribe quality was poor. We are still awaiting another vendor's laser for evaluation.

2.3 Substrate Cost Reduction

The largest single material cost for our photovoltaic manufacturing technology is the polyimide substrate. In an effort to reduce this cost we evaluated thinner polyimide and films as substrate material. We evaluated both one mil and ½ mil material for comparison with our standard two mil material. Critical issues were the ability of the thinner substrate to hold up in our roll based deposition systems and the dimensional stability of the substrate in our patterning processes.

Both the one mil and ½ mil material performed adequately in our roll based deposition systems after minor adjustments in web tension. Sensitivity to web tension and web feed were particularly high for the ½ mil material.

Adapting the printing and laser scribing systems to the thinner substrates was more of a problem. Both the web drive systems and vacuum pull down systems required modification. Without careful control, the thinner substrate tended tocrease. Proper sequencing of the vacuum pull down was found to prevent this. Adaptations have made it possible to use one mil material reliably. We have, however, found that the ½ mil material is structurally too weak to be used reliably in the large-scale manufacturing environment.

The end result of this effort was to develop the capability of using one mil polyimide substrate in our manufacturing process. This effectively cuts the substrate cost by 50%.

2.4. Busbar Attachment and Web Cutting Automation

Roll-based laminating technologies

ITF evaluated the potential of existing roll-based laminating technologies and equipment taking into account versatility and capacity. The initial vendor survey revealed that currently no manufacturer has an OEM type laminator that can be directly implemented into Iowa Thin Film's production line. Most systems are designed for single sheet feed. ITF's requirements call for a roll to roll lamination system, where a feed stock of modules on a roll can be loaded on to the laminator, encapsulated, then rolled up on a take up mandrel. However, several manufacturers offer base units that can be modified to fit ITF roll based laminating requirements.

Two types of roll based lamination techniques were identified. One is Thermal Set Adhesive, "TSA," and the other is Pressure Sensitive Adhesive, "PSA." Nip rolling TSA's can be done on a roll laminator as long the adhesive's cure time is relatively short. Using heated nip rollers with friction tensioners on the rolls of raw material, thin TSA's can be roll laminated. Thicker TSA's (>15 mil) using Ethylene Vinyl Acetate (EVA) as the thermal set adhesive cannot be roll laminated because of the relatively long cure time. However, it is possible to seal thicker TSA encapsulated modules with a roll laminator, cut the modules to length, then place a series of modules in a press, and bake the entire stack until cured.

The lamination of PSA's requires a completely different system. PSA lamination requires standard non-heated nip rollers. The top roller needs to be a rubber coated roller with a durometer in the area of 60-100. Different lamination materials will probably require changing the durometer of the upper roller. The lower roller should be made of a rigid material. The rollers described are designed for laminating thin materials (less than .005"). A steel upper roller can be used with a thicker (greater than .018") laminate and adhesive combinations. The reason for this difference in thickness of materials is due to the presence of busbars. Thicker materials conform around the busbar which eliminates air bubbles. The thinner material doesn't. For this reason a different top roller is necessary. A softer upper roller will conform the thinner laminate and eliminate air bubbles next to and around the busbars. A softer upper roller may work with a thicker laminate but there are no >20 mil film UV resistant PSA's available.

Busbar attachment and Web Cutting Automation

Another accomplishment towards improving the manufacturability of the ITF solar modules was to evaluate and then develop automated equipment to implement an automated system for busbar attachment and cutting modules off the roll.

Busbar attachment After reviewing the existing market for attaching busbars to the web, two system types were identified. The first is for Tefzel/EVA. This type of system would use robotics to assemble the module, there were multiple vendors available with robotic arms to fit this function. The robotic arm would also be able to apply both the conductive adhesive to the web, which holds the busbar in place, and the busbar to the web. Many vendors specialize in making custom heads for robotic arms. However, this procedure results in sheets of material being processed one at a time with the web being cut and placed in a jig or fixture. The robotic assembly would then occur placing conductive adhesive and busbar to the cut sheet. After the robotic assembly was completed the operator would have to change out the fixture for another sheet and start the robotic over again. The operator could complete the module encapsulation by placing the cosmetic tape over the busbars and sheet the module with Tefzel/EVA overlaminate. The module would then be removed from the fixture and laminated in a conventional vacuum laminator. This would complete the module assembly. The possibilities of accomplishing this task roll-to-roll would be impossible because of the physical connection between the busbar and the material. The bus would fall or break off of the web before lamination when the material was rolled up. Additionally, this system does not address the need to interconnect the modules on the web. This system would also leave the problem of making the ½" weather seal that is required for individual modules to pass the twenty year lifetime testing.

The second system is a taping system where conductive copper tape is placed on the contact pads. Most of the taping industry is geared around cutting and feeding a piece of tape so an operator can pick the piece of tape and place it where it needs to be. Another part of the industry is geared around taping large rigid structures as in the box industry. However, one manufacturer was found that has a taping system which can do sheet taping. Their machine can place strips of tape lengthwise across a thin piece of material. As a self contained unit it is designed to do sheets of material one at a time. The heads for this unit can be purchased individually for alternative uses. With a system like this it is possible to place busbar material across the web in a roll-to-roll fashion. If this system is used with a alternative encapsulation (other than Tefzel) like a TSA/UV stabilized polyester then, it can be roll laminated.

Web Cutting Automation A survey of vendors of equipment for cutting off module lengths for encapsulation was conducted. There are many manufacturers that make dies and presses for cutting off length of material for encapsulation. Some of the die types include rotor die, clicker die, and die cutting. This industry is geared around cutting raw material in multiple forms then processing the cut assemblies while still held in the web. Die-cutting ITF's photovoltaic material requires precision die-cutting: the equipment has to be able to cut the modules within a half of a millimeter. One manufacturer was found that offered precision placement and die-cutting in a package that can process our material. This system is fairly expensive incorporating optical alignment with precision die cutting. The other two process for cutting out the material were clicker die and rotary die. Both offer high speed and through put, but precision is not possible without perfect module to module fabrication. Any variation in the distance between modules could result in cutting the wrong area. Both of these systems are based on simultaneous cutting and advancing the material. Die cutting offers the most flexibility in terms of accuracy and throughput for processing ITF's photovoltaic cells.

The final automated systems designs

The final design for the automated busbar attachment system and the sheeting/die cutting system consists of a base system with the following features. The base system consists of a supply and take up mandrel that are compatible with the ITF a-Si on a polymer substrate production line. These mandrels are used for handling the solar cell material through either system. A torque motor/controller is on the take up mandrel and a stepper motor/encoder is on the supply mandrel. These two systems give precision control of the web in the X direction or down the web. The Y direction of the web is controlled by a linear screw type drive system that the frame for the supply mandrel is attached to. It consists of a carriage plate, which supports the supply roll. This carriage is mounted on four pillow block bearings. The bearings ride on two shafts. These shafts are mounted to a base plate by base supports. A short acme screw drives the carriage plate along the Y axis. A feedback controlled linear motor drives the screw along the Y axis. Feedback for the controller comes from linear optical sensors that detect the edge of the web. The rotation or Theta axis adjustment is done manually by separate mechanical adjusting systems for both the busbar attachment and the sheeting die-cutting systems. Automation is not necessary for the rotational axis, as once the carriage plate is aligned along the Theta, there is no need to realign the system during the run. Occasional adjustments are required from run to run. The controller for alignment and cycling either sheeting/die-cutting or busbar taping operation is done by the X axis drive controller This is a multifunction controller with multiple inputs and outputs.

Busbar attachment system For the busbar attachment system, the base system is configured with a platen that has the taping heads for placing the conductive bus onto the web. The taping heads are placed down on the web where they travel across the platen, placing the conductive busbar on the web. A vacuum holddown platen is used to assure that there is no web movement during the tape application process. At the end of each stroke the heads cut the tape and lift off the web. The lift off of the heads is accomplished at the end of each stroke by two air cylinders. This enables the heads to return to the beginning of the stroke without touching the web. Sensors for the lift up of the tape heads are mounted at each end of the tape heads stroke. These sensors are adjustable for different lengths of tape, moving the sensors varies the start and stop position thus changing the overall length of tape that is applied to the web. After tape placement is completed the web is advanced for the next busbar placement location, during web advancement the taping heads are returning to their original position. The process is repeated in processing all of the solar modules on the given length of web.

Sheeting/die-cutting system For the sheeting/die-cutting system, the base system is mounted around the press, where the take off height of the web will be slightly higher than the base of the die. The process is similar to the busbar system. The web is aligned relative to the press. Once the web is aligned, the press cycles and the solar material is cut to specification. Optical sensors are used to verify the location of the modules on the press before the die-cutting press cycles. Small tabs are used to hold the modules in the carrier web for extraction from the web down line. Once the press is cycled, the web is advanced to the next solar module where the optical sensor will realign and the press cycle will be repeated. This process is repeated until all modules on the web have been die cut and extracted from the carrier web.

2.5. Reduction in Encapsulation and Module Assembly Costs

In the effort to reduce module assembly costs, ITF established a roll based manufacturing process to decrease module assembly labor costs. In an effort to reduce the cost of the single layer of high-cost fluoropolymer encapsulant, ITF identified a low-cost top transparent encapsulant to replace it. Evaluation of encapsulant performance included effects on module performance, adequacy for edge sealing, and stability against temperature cycling. In addition, ITF investigated multiple layers of lower cost transparent polymers as possible replacements for the high cost material, Tefzel®, that was in use.

Thermal roll lamination system

A thermal roll lamination system for use with laminates uses a hot shoe preheater system. This system can encapsulate pre-assembled modules (with copper busbar on the ends) that are fed into the roll laminator sequentially. Because of the limited nip time of roll laminating, Dupont's Tefzel® with 18 mil EVA cannot be cured using this system. An additional curing method is required after sealing 18 mil EVA on a thermal roll lamination system. ITF test results showed that the best roll laminating performance came from laminating thin TSA's with the hot shoe type preheater system.

Three systems were tested. The first system involved assembling modules with busbars attached to the sides. Next the cells were sealed on the thermal roll laminator, then cured in a press and in an oven. Two techniques were tried for curing. One involved laminating only a single module in the press, then curing it in a oven. The second involved laminating a series of modules in the laminator, stacking the layers in the press and baking them until the EVA was cured. The second system involved using a frame and bladder to seal the module, placing the entire frame into an oven, and baking it until the EVA was cured. These modules were not pre-rolled in the roll laminator. They were simply assembled, placed under the bladder, pumped down, and baked. The third system used the same assembly as the second but instead of a frame and bladder a backing sheet of aluminum and high temperature vacuum bag were used. The module is assembled on a sheet of aluminum and then the entire module/sheet is slipped into a large vacuum bag, pumped down, and held in an oven until the EVA is cured.

Comparison of the three lamination systems The roll laminated module lost some clarity due to scratches that were generated during the roll laminating process. However, the single layer group still looked better than the multiple layer group. Small wrinkles formed on the back of the multiple layer group. These may have been caused by uneven roll lamination: the EVA had a tendency to bunch up and press down the web when it went through the rollers. To correct for this, a minimum pinch distance is required to accommodate the thicker EVA.

The vacuum lamination technique produced very clear modules. However, they were also very uneven in thickness indicating uneven pressure in the laminator. This was resolved by adding an offset base to accommodate for bladder stretch during pump down. The vacuum bag provided the best test results: the modules were very clear and very flat. However, there are no commercially available high temperature vacuum bags, making this process very difficult to do in large quantities. Multiple laminations are possible in vacuum bags, thereby decreasing cycle times.

The following was learned regarding roll laminating other materials such as pressure sensitive adhesives and thin thermal set adhesives. The process steps include: 1) placing conductive metal foil tapes down on the module bus area; 2) laminating in the roll laminator with shoe preheater; and 3) cutting and testing modules. This process roll laminating provides the best results in terms of "ease of manufacturability."

The majority of the encapsulants tested to date are listed in Table 4. Each is rated as "pass" or "not pass" for the following in-house tests: salt water corrosion, 80ºC soak, and thermal cycling (-40ºC to 80ºC). UV soak and optical transmission tests for the encapsulants that passed all three tests are presented below Table 4.

Table 4. Results of in-house testing, conditions pass/fail.

Film/Adhesive/Test	Saltwater Corrosion	80ºC soak	Thermal Cycling
Tefzel®/EVA	pass	pass	pass
Tefzel®/Silicon PSA	pass	pass	pass
Tefzel®/Acrylic PSA	fail penetrated module	pass	fail delaminated
Dartek®/Eva	pass	pass	pass
Dartek®/silicone PSA	pass	pass	pass
Dartek®/Acrylic PSA	fail penetrated module	pass	pass
Acalar®/Acrylic PSA	failed delaminated	fail cracked	fail cracked
Polyester/Polyethylene #12	pass	pass	pass
Polyester/Polyethylene #23	pass	pass	pass
Polyester/Polyethylene #28	pass	pass	pass
Tedlar®/EVA	pass	pass	pass
Tedlar®/Silicone PSA	fail delaminated	pass	pass
Tedlar®/Acrylic PSA	fail delaminated	pass	fail delaminated

These modules were not sent to NREL for UV exposure due to the amount of time the test took and the availability of films that were wide enough at the time the other modules were sent in: Tedlar®/ EVA and Tefzel®/silicone PSA were not sent because the sample films were not wide enough for the ft^2 modules that NREL requested for testing; Polyester/Polyethylene #23 wasn't sent because two previous candidates, #12 and #28, had been sent; and Tefzel®/EVA has already passed IEEE module qualification sequence Standard 1262. Dartek®/EVA wasn't sent in for UV testing because the initial Dartek® module failed the UV exposure testing. The Tedlar®/EVA and Tefzel®/silicone PSA samples were sent to NREL for UV testing.

Three candidate lamination material samples encapsulating $1ft^2$ single junction a-Si modules were sent to NREL for UV exposure testing. The intention of this experiment was to see how these experimental encapsulants would respond under UV exposure levels as specified in the IEEE sequence Standard 1262. The modules were exposed for 35.1 days at a UV irradiance of 17.8 W/m2. This exposure simulates total exposure of 54 MJ/m2, and approximate lifetime UV exposure of 10 years under normal irradiance. The modules that were sent to NREL were not state-of-the-art modules but typical 4 to 4.5 percent efficient modules.

After receiving and examining the results of the optical transmission tests provided by NREL (Table 5), we noted that the majority of the losses in Pmax (approximately 10%) were due to the Staebler-Wronski effect. F24 showed the greatest overall losses, apparently due partly to yellowing of the non-UV-stabilized nylon film that was used in the encapsulant.

After receiving the modules that had been UV soaked by C.R. Osterwald at NREL, optical transmission data was taken on the encapsulants. F22 and F23 were polyester/polyethylene encapsulants, with different thicknesses of film and adhesive. F24 was the nylon/silicone encapsulant. Data taken above 600nm on F22 had too much noise to get an accurate number for the percent change of pre-UV soaked encapsulant and post-UV soaked material. The encapsulants that were tested, cut from the trimmed material (pre-UV soaked) and from the weather seal (1/2" border) post-UV soaked material, provided the data shown in Table 5.

Table 5. Relative changes in I-V parameters (%): data from NREL test results.

ID	V_{oc}	I_{sc}	FF	P_{max}
F22	-0.7	-5.9	-2.1	-8.7
F23	-2.1	-4.0	-8.1	-14.6
F24	-0.7	-12.2	-4.7	-18.3

The differences in percentage change in the light transmission of the pre-UV soaked and post UV-soaked material is shown in Table 6.

Table 6. Relative changes in light transmission (%) as tested at ITF.

ID	400nm	450nm	500nm	550nm	600nm	650nm	700nm	750nm
F22	-13.0	-0.7	0.0	0.0	---------	---------	----------	----------
F23	-16.0	-2.4	-1.7	+0.5	+0.6	+1.1	+1.9	+1.1
F24	-38.4	-18.7	-8.8	-3.8	-1.5	-0.8	-0.8	-0.4

For the polyester/polyethylene encapsulated modules the greatest losses occurred between 350nm and 450nm. Considering the amount of light energy available at frequencies below 400nm the losses of 13-16% seem quite negligible. It was interesting to see that there was an increase in the percentage of light transmitted from 550nm to the end of the visible light spectrum at 750nm. F24 seemed to suffer the greatest losses in light transmission throughout the entire visible spectrum. Part of these losses was due to the fact that the encapsulated film used was a non-UV stabilized nylon film. Again the majority of the losses occurred between 350nm and 500nm. Table 6 only lists percentage change in the visible spectrum. Data on all three samples shows very little difference in pre- and post-exposure above 750nm and below 250nm. The polyester/ polyethylene encapsulants look promising for a medium lifetime product (up to 10 years).
In a further effort to provide a lower cost encapsulant, candidate stacks were tested for both lamination properties and adequacy of physical protection. Tests carried out included temperature cycling, heat/humidity, UV degradation, and abrasion.

The test results presented in Table 7 indicate that two composite laminates were viable candidates. The first viable composite laminate consists of a stack of 3 mil UV stabilized polyester, 2 mil polyethylene, 2 mil solar module, 2 mil polyethylene, and 3 mil polyester. The second composite laminate consists of a stack of 1.5 mil Tefzel, 5 mil EVA, 2 mil solar module, 5 mil EVA, and 1.5 mil Dartek. Item #3 in the table refers to the Tefzel/EVA/A-Si PV/EVA/Dartek, and item #7 refers to the Polyester/Polyethylene/ A-Si PV/Polyethylene/ Polyester composite.

The two modules represent different aspects of encapsulation. Item # 3 represents a long lifetime module while lowering the costs over traditionally encapsulated modules. Item # 1 provides excellent durability, UV resistance, temperature variance, resistance to abrasion and heat/humidity extremes, while lowering the cost of the more traditional. Item # 7 represents a fairly durable UV resistant module with great resistance to heat/humidity and temperature cycling. With the lifespan of the encapsulation ranging between 5 to 10 years, this is an intermediate encapsulation designed for shorter life applications. The best in terms of its low cost and ease of manufacturing, item # 7 is roll-to-roll laminated, tens of feet per minute, and item # 3 is vacuum laminated, a few feet per hour. Both types of encapsulation fill different needs in the

Table 7. Research results indicating viable composite laminate candidates.

Item #	Top Film	Top Adhesive	Bottom Adhesive	Bottom Film	Durability	UV Resistance	Temp. Cycling	Heat/Humidity Soak	Resistance to Abrasion	Cost
1	1.5 mil Tefzel	18 mil EVA	18 mil EVA	1.5 mil Tefzel	5	5	5	5	5	5
2	1.5 mil Tefzel	5 mil EVA	5 mil EVA	1.5 mil Tefzel	4	5	5	5	5	5
3	1.5 mil Tefzel	5 mil EVA	5 mil EVA	1.5 mil Dartek	4	5	5	5	5	3
4	1.5 mil Tefzel	18 mil EVA	5 mil EVA	1.5 mil Dartek	4	5	5	5	5	4
5	1.5 mil Dartek	18 mil EVA	18 mil EVA	1.5 mil Dartek	5	1	5	5	2	2
6	1 mil Polyester	2milPoly-ethylene	2milPoly-ethylene	1 mil Polyester	2	2	4	4	3	1
7	3 mil Polyester	2milPoly-ethylene	2milPoly-ethylene	3 mil Polyester	3	3	5	5	3	2
8	2 mil Polyester	8milPoly-ethylene	8milPoly-ethylene	2 mil Polyester	4	4	5	5	3	3
9	2 mil Polyester	8milPoly-ethylene	2milPoly-ethylene	3 mil Polyester	4	4	5	5	3	3
10	4 mil Polyester	6milPoly-ethylene	6milPoly-ethylene	3 mil Polyester	4	4	5	5	3	3

PV industry. There is no one perfect encapsulation for all situations. All composite materials supplied for these tests were assembled by outside purveyors.

Use of roll laminating in conjunction with the new laminant results in a 90% reduction in material cost and a 95% reduction in labor costs.

2.6 Automated Module Testing

An automated module tester was designed, assembled and tested. The purpose of this tester was to increase the throughput of module testing, improve accuracy, and reduce labor cost. Following evaluation of a number of module transport mechanisms, a vacuum pickup arm technology it was chosen. The tester uses a solenoid driven pivot arm to process five groups of modules simultaneously. Five separate vacuum chucks connected to a pivot arm pick up modules from the supply stacks and move them to an illuminated test station. Contact probes rotate into place for testing of the modules. A single data acquisition card (DAC)is used to take data on the five modules. A second arm picks the modules from the test location and moves each to the pass or fail bins depending on the individual test result. During this movement, a new group of modules is moved to the test location.

For the first evaluation, three runs of approximately 10,000 modules were put through the new "autotester." During this initial testing period several problems were identified in the calibration technique, the module supply holders, and the pads used for making contact with the solar panels. Subsequent adjustments were made-the most notable being in the calibration technique.

Calibration technique It was initially thought that the best calibration technique would be to place a known reference module over each of the five light zones and adjust the light sources until each of the zones was calibrated to the known reference module. However, this was shown to be an impossible task given the light source. After some experimenting, the decision was made to place a calibrated module of known current in each of the five zones. The DAC would then gather data from each of the five "new" modules to be tested and compare the data it received with that of the known calibrated modules and thus generate a correction coefficient data array. This correction coefficient was used to adjust the data received from the DAC during testing to calculate the actual output of each "new" module tested.

Subsequent testing of this technique has shown this method to be quite accurate. Data received from the DAC for a particular module is compared with its actual power point. Accuracy has been determined to be good to one tenth of a milliampere.

Analysis

Two aspects were examined in comparing the new module tester operation with manual testing. The first was "test rate", and the second was accuracy as compared to hand measurement and yield loss evaluated as "testing accuracy" and "placement accuracy."

Test rate: A single operator manually testing modules can test about 900 modules a hour, assuming the material being tested is about 80% "passing or better". The automated tester can test approximately 2,700 modules per hour assuming the material being tested is about 80% "passing." This number falls to about 1,900 modules per hour when the material is about 50% "passing." The reason for this is that every module that fails the first time through is re-tested at a slightly lower spec. A manual testing system can only test approximately 600 modules per hour with 50% "passing," depending on the operator. The operator of a manual system has the ability to place modules into more than two categories. The autotester can only place modules into two categories.

Testing accuracy: The autotester has proven significantly better in terms of testing accuracy. The computer driven tester will not accidentally place a failing module into the "passing" bin. It will however place a passing module in the "failing" bin, not because it was failing, but because of an error in handling, e.g., poor contact or a module in backwards. With the automated tester, we have not yet found a single bad module in the "passing" bin. In comparison, we have found with manual testing large quantities of bad modules in the "passing" bins, due to operator error intensified by hours of repetitive testing.

Placement accuracy: For placement accuracy, the autotester again has proven superior. A manual tester can test a module and know that the module is in a certain category but accidentally place the module in the wrong stack because of being tired, confused, or distracted. The autotester will not accidentally place a module in the wrong bin. Of the modules re-tested in the "passing" bin there has not been found one bad module.

However, we initially found quantities of "good" modules in the "failing" bin. When we first re-tested modules the autotester had rejected, we initially found approximately 50% of these modules in the "failing" bin to be in two categories: 20% passing (above spec.) and 30% just below spec (90% of passing current). After a few modifications to the pressure pads of the tester and modifying the module feed area, these numbers improved. Approximately 20% of the modules in the "fail" bin were passing (down from 50%). Of these, 5% were passing (above spec) and 15% were just below spec (90% of passing current).

Comparison of test rate, testing accuracy and placement accuracy may be summarized as follows:

	Hand Testing	**Automated Testing**
Test Rate	900 modules/hr.	2,700 modules/hr.
Testing Accuracy	Several types of repeated errors	100% "passing" modules were "passing"
Placement Accuracy	Several types of repeated errors	100% "passing" in "passing" bin 20% of modules in "failing" bin were "passing"

3.0 CONCLUSIONS

Iowa Thin Film Technologies has completed the three phase program which has increased throughput and decreased costs in nearly all aspects of its thin film photovoltaic manufacturing process.

The overall manufacturing costs have been reduced to by 61 percent through implementation of the improvements developed under this program.

These developments have significantly improved the cost-effectiveness of this Thin Film photovoltaic technology. This has moved the technology forward to the point where it is commercially viable.

REPORT DOCUMENTATION PAGE

Form Approved
OMB NO. 0704-0188

1. AGENCY USE ONLY (Leave blank)

2. REPORT DATE
March 2000

3. REPORT TYPE AND DATES COVERED
Final Technical Report, 5 July 1995–31 December 1999

4. TITLE AND SUBTITLE
Photovoltaic Manufacturing Technology Monolithic Amorphous Silicon Modules on Continuous Polymer Substrates; Final Technical Report, 5 July 1995–31 December 1999

5. FUNDING NUMBERS
C: ZAF-5-14271-4
TA: PV006101

6. AUTHOR(S)
F. Jeffrey

7. PERFORMING ORGANIZATION NAME(S) AND ADDRESS(ES)
Iowa Thin Film Technologies
2337 230th St.
Boone, IA 50036

8. PERFORMING ORGANIZATION REPORT NUMBER

9. SPONSORING/MONITORING AGENCY NAME(S) AND ADDRESS(ES)
National Renewable Energy Laboratory
1617 Cole Blvd.
Golden, CO 80401-3393

10. SPONSORING/MONITORING AGENCY REPORT NUMBER
SR-520-27960

11. SUPPLEMENTARY NOTES
NREL Technical Monitor: R.L. Mitchell

12a. DISTRIBUTION/AVAILABILITY STATEMENT
National Technical Information Service
U.S. Department of Commerce
5285 Port Royal Road
Springfield, VA 22161

12b. DISTRIBUTION CODE

13. ABSTRACT *(Maximum 200 words)*
Iowa Thin Film Technologies is completing a three-phase program that has increased throughput and decreased costs in nearly all aspects of its thin-film photovoltaic manufacturing process. The overall manufacturing costs have been reduced by 61 percent through implementation of the improvements developed under this program. Development of the ability to use a 1-mil substrate, rather than the standard 2-mil substrate, results in a 50 percent cost-saving for this material. Process development on a single-pass amorphous silicon deposition system has resulted in a 37 percent throughput improvement. A wide range of process and machine improvements have been implemented on the transparent conducting oxide deposition system. These include detailed parameter optimization of deposition temperatures, process gas flows, carrier gas flows, and web speeds. An overall process throughput improvement of 275 percent was achieved based on this work. The new alignment technique was developed for the laser scriber and printer systems, which improved registration accuracy from 100 microns to 10 microns. The new technique also reduced alignment time for these registration systems significantly. This resulted in a throughput increase of 75 percent on the scriber and 600 percent on the printer. Automated techniques were designed and implemented for the module assembly processes. These include automated busbar attachment, roll-based lamination, and automated die cutting of finished modules. These processes were previously done by hand labor. Throughput improvements ranged from 200 percent to 1200 percent, relative to hand labor rates. A wide range of potential encapsulation materials were evaluated for suitability in a roll lamination process and for cost-effectiveness. A combination material was found that has a cost that is only 10 percent of the standard EVA /Tefzel® cost and is suitable for medium-lifetime applications. The 20-year lifetime applications still require the more expensive material.

14. SUBJECT TERMS
photovoltaics ; Photovoltaic Manufacturing Technology ; PVMaT ; module manufacturing ; systems integration ; deposition process ; substrates ; throughput

15. NUMBER OF PAGES

16. PRICE CODE

17. SECURITY CLASSIFICATION OF REPORT
Unclassified

18. SECURITY CLASSIFICATION OF THIS PAGE
Unclassified

19. SECURITY CLASSIFICATION OF ABSTRACT
Unclassified

20. LIMITATION OF ABSTRACT
UL